ACS Sustainable Chemistry & Engineering

Research Article

pubs.acs.org/journal/ascecg

Functionalized Carbon Spheres for Extraction of Nanoparticles and Catalyst Support in Water

Jitendra Kumar,[†,‡] Ramakrishna Mallampati,[†,‡] Avner Adin,[†] and Suresh Valiyaveettil*[,‡]

[†]NUS Environmental Research Institute, National University of Singapore, T-Lab Building, 5A Engineering Drive 1, Singapore 117411

[‡]Department of Chemistry, National University of Singapore, 3 Science Drive 3, Singapore 117543

Supporting Information

ABSTRACT: Increased use of nanomaterials in commercial products will lead to environmental contamination in the near future. So far, limited adsorbents are available for the removal of such emerging pollutants from water. The objective of this work was to synthesize functionalized carbon nanospheres (C-spheres) for the removal of emerging nanopollutants from water and to study the mechanisms involved. C-spheres were prepared using hydrothermal carbonization of glucose. Post-modification with polyethylenimine (PEI) generated amine-coated C-spheres, followed by protonation using diluted acid solution. The surface functional groups and morphologies of the C-spheres were characterized using infrared spectroscopy and field emission scanning electron microscopy, respectively. The C-spheres were used for the extraction of citrate-capped gold and silver nanoparticles from water. The equilibrium adsorption data was interpreted using Langmuir and Freundlich isotherms, and the adsorption mechanism was investigated using kinetic studies. Our data suggest that the adsorption of nanoparticles on modified C-spheres followed pseudo-second-order kinetics, and adsorption can be best explained by the Langmuir adsorption model. The observed results suggest that the developed material shows enhanced extraction capacities (102 mg/g for AuNPs and 135 mg/g for AgNPs). Further, the NP-adsorbed C-spheres were evaluated for the catalytic reduction of *p*-nitrophenol to demonstrate the activity of adsorbed NPs.

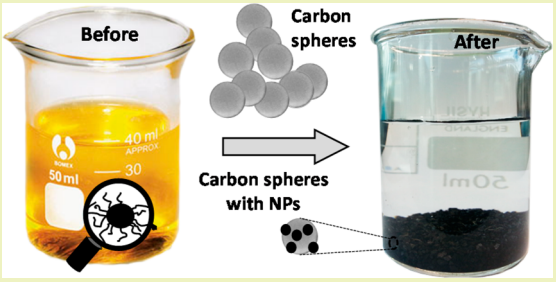

KEYWORDS: *Carbon sphere, Nanoparticles, Adsorption, Hydrothermal, p-NP reduction, Water treatment*

INTRODUCTION

Engineered nanoparticles are interesting due to their unique electro-optical, antimicrobial, magnetic, and catalytic properties, and they have found many applications in biosensing[1] and antimicrobial products,[2] some of which in water treatment.[3] As the number of consumer products incorporated with nanomaterials increase, there is a growing concern regarding environmental contamination, followed by the adverse impact on living organisms.[4−11] Even though, there are many reports on *in vitro* and *in vivo* studies of toxicity induced by nanoparticles, a detailed mechanism of such toxicity is not fully understood.[12−14] Hence, engineered nanoparticles are considered as an emerging class of contaminant with a potentially wide distribution and end up in the water through various pathways.[15,16] Thus, it is important to address the issue of environmental remediation of nanoparticles to prevent health hazards from long-term exposure to nanoparticles.

Many purification technologies have been developed to remove pollutants from water; however, only a few reports exist on studies related to the removal of nanoparticles, which includes coagulation, membrane filtration, and aggregation.[17−19] The current water treatment methods are not efficient for the removal of nanoparticles owing to small size and high stability. Different adsorbents including polymers, metal oxides, activated carbon, and hybrid materials were used for the removal of nanoparticles, which showed different adsorption capacities based on various factors.[20−24] The hydrothermal carbonization technique generates interesting carbon materials, which can be used for the removal of cationic, anionic, and organic pollutants with encouraging results owing to high stability and low toxicity.[25−30] However, use of these carbon materials for the removal of nanoparticles from water has not been evaluated. Synthesis, functionalization, and adsorption properties of C-spheres prepared from hydrothermal carbonization of saccharides, glucose in particular, has been well documented.[25−30] The adsorption of nanoparticles using carbon derived from natural sources can be considered as an eco-friendly and cost-effective alternative for the wastewater treatment process.

Previously, the authors reported novel adsorbent materials for water remediation capable of removing a range of pollutants including nanoparticles.[22,23,31,32] The general aim of this work is to develop an easy and scalable process to develop functional materials for the removal of nanoparticles from water. The

Received: July 3, 2014
Revised: October 12, 2014
Published: October 22, 2014

specific goals herein include synthesis of C-spheres using hydrothermal carbonization of glucose and its post-modification with polyethylenimine (PEI) for the removal of negatively charged AgNPs and Au NPs and to demonstrate the retention of catalytic activity of nanoparticles after adsorption on modified C-spheres, which is summarized in Scheme 1.

Scheme 1. Extraction of NPs by C-spheres and Catalytic Conversion of *p*-NP to *p*-AP by NPs Adsorbed on Carbon Material

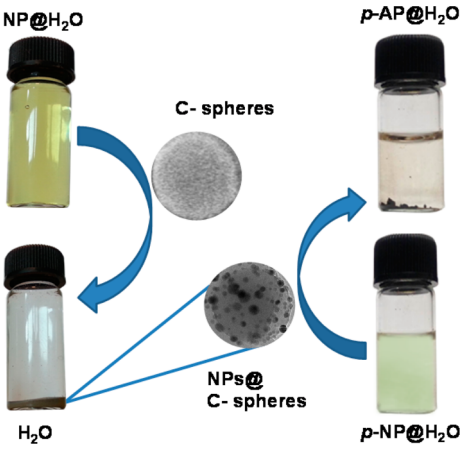

MATERIALS AND METHODS

Materials. Stock solutions of AuCit and AgCit were prepared according to a modified procedure (Cit is used as abbreviation for citrate throughout the manuscript).[33,34] All chemicals and reagents used were AR grade and purchased from Sigma-Aldrich.

Synthesis of C-spheres. Glucose was carbonized under hydrothermal conditions to obtain the C-spheres. Typically, 5 g of glucose was suspended in 50 mL of water in an autoclave and heated at 200 °C for 12 h. The black suspension obtained was washed with methanol (100 mL) and water (100 mL) until the filtrate becomes colorless. The C-spheres were dried under vacuum, characterized, and used for surface functionalization with polyethylenimine (PEI).

Surface Functionalization of C-spheres. The C-spheres (1.2 g) were suspended in water (100 mL), and PEI (5.0 g) was added to the solution. The mixture was stirred at 60 °C for 12 h, followed by filtration and washing the residue with ethanol (100 mL) and water (50 mL) to yield PEI-coated C-spheres (C-PEI, 1.0 g), which were suspended in water (90 mL) and mixed with glutaraldehyde (9 mL, 50% v/v H_2O) for cross-linking the PEI. The mixture was stirred overnight, filtered, washed with ethanol (100 mL) amd water (50 mL), and dried to get glutaraldehyde cross-linked material (C-PEI-Glu). Finally, the isolated C-PEI-Glu was suspended in 20 mL of 1 M HCl, stirred for 15 h, filtered, and washed with water (200 mL) until the filtrate became neutral. The protonated material was dried under vacuum for 4 h, which afforded 1.0 g of material (C-PEI-GluH$^+$) and used for the nanoparticle adsorption studies in subsequent experiments.

Synthesis of Nanoparticles. $AgNO_3$ (0.1 M, 1.25 mL) and tribasic sodium citrate (0.05 g) were dissolved in water (195 mL). A fresh solution of $NaBH_4$ (0.01 g) in water (2 mL) was added dropwise into the above solution. Immediately, the color of the solution turned gray, which indicated the formation of nanoparticles. The solution was stirred for 24 h and diluted to 200 mL with distilled water. Similarly, $KAuCl_4$ (0.1 M, 0.5 mL) was used for the synthesis of AuCit nanoparticles keeping all other steps the same, and the red color solution obtained was diluted to 200 mL with distilled water. Both nanoparticle solutions were used for extraction experiments by diluting the stock solution with water to get the desired concentrations. The absorption spectra were recorded at 520 and 390 nm for AuCit NP and AgCit NP, respectively, which is consistent with the earlier reports.[33−35]

Characterization of Materials. Field emission scanning electron microscopy (JEOL JSM-6701F) in conjunction with energy dispersive X-ray spectroscopy (EDS) was used to probe the morphology and chemical composition of the material, respectively. The IR spectra were recorded on a Bruker ALPHA FTIR spectrophotometer using a standard KBr pellet. Quantitative analysis of the materials was

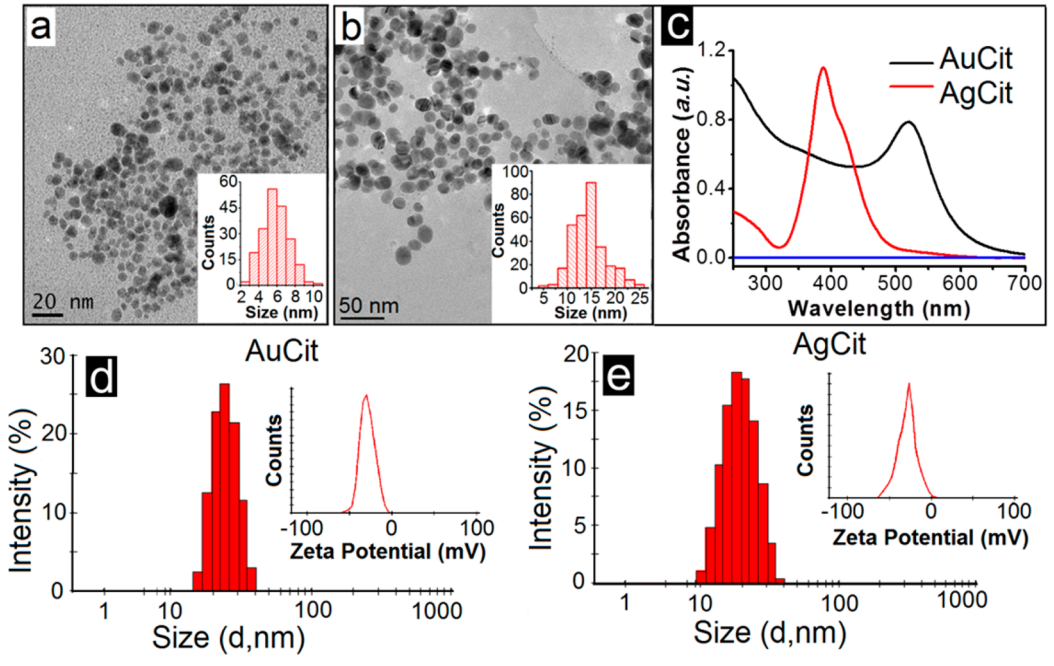

Figure 1. TEM image of (a) AuCit and (b) AgCit NPs (inset shows the size distribution). (c) UV−vis spectra of nanoparticle solution (AgCit solution was diluted eight times before taking the spectra. Size distribution of AuCit (d) and AgCit (e) nanoparticles (corresponding inset shows zeta potential of NPs).

dx.doi.org/10.1021/sc5004242 | ACS Sustainable Chem. Eng. 2014, 2, 2675−2682

performed using a dual view optima 5300DV ICP−OES system. The CHN analysis was done using an Elementar Vario Micro Cube elemental analyzer. The morphologies of NPs were observed using JEOL 2010-F field emission transmission electron microscope (FETEM). Size and zeta potential measurements of synthesized NPs were done using a Malvern Zetasizer Nano-ZS90. The software use non-negative least-squares (NNLS) analysis for size distribution data and Henry's Function F for zeta potential measurements. Complete analysis of size and zeta potentials of all materials (adsorbates and adsorbent) are given in the Supporting Information. We used ultrapure water as the dispersant in both size and z-potential measurements. The pH of the solutions used was 6.5. We did not use any salt to study the role of ionic strength on adsorption as these salts tend to destabilize the nanoparticles. We maintained pH 6−7 for all adsorption experiments in consideration with the NP stability. The quantitative measurement of NP concentration was done by comparing the absorption maxima with the standard solutions on a UV−vis spectrophotometer (Shimadzu −1601 PC spectrophotometer).

Kinetic and Isotherm Studies. Appropriate amounts of adsorbent (0.02 g) were added to the NP solutions (9 mL) of specific concentrations. All adsorption experiments were carried out at room temperature (25 °C) using an orbital shaker at 300 rpm for 6 h. In case of time dependent studies, the residual NP concentrations were analyzed after a predetermined time intervals, and the amount of NP adsorbed at equilibrium Q_e (mg/g) was calculated using eq 1.[36]

$$Q_e = (C_0 - C_e)\frac{V}{M} \quad (1)$$

where C_0 and C_e (mg L^{-1}) are initial and equilibrium concentrations of adsorbates, respectively, V is the volume of the solution, and M is the weight of the adsorbent used. The concentrations of NP solutions used for the extractions were in the range of 5−60 mg/L.

RESULTS AND DISCUSSION

The adsorbent material (C-spheres) was synthesized using hydrothermal carbonization, which was modified as described in the Materials and Methods section. The silver and gold nanoparticles were synthesized, fully characterized, and used for adsorption experiments. The NPs were observed under TEM to determine the size (Figure 1a and b), and all NPs showed a size range of 5−25 nm. In the UV−vis spectra, the absorption maxima (λ_{max}) of the NPs were observed at 520 and 390 nm for AuCit NP and AgCit NP, respectively (Figure 1c), which is consistent with the literature reports.[33−35] Further characterization of NPs was done using a Zetasizer instrument where the size and zeta potential of the NPs were measured. The average hydrodynamic size in water was 26.4 ± 0.4 nm for AuCit NPs and 26.6 ± 0.4 nm for AgCit NPs (Figure 1d and e). The zeta potential values were −30.0 ± 0.2 and −29.1 ± 0.2 mV for AuCit and AgCit NPs, respectively (Figure 1d and e).

After hydrothermal carbonization, the C-spheres were isolated by filtration and dried. The surface functional groups on the C-spheres were identified using FT-IR spectra recorded in the range of 4000−400 cm^{-1} (Figure 2). The spectra before and after functionalization of C-spheres are almost similar without significant changes. The broad band in the range of 3200−3600 cm^{-1} for C-spheres can be attributed to the O−H stretching vibrations of the hydroxyl groups and/or the carboxyl groups. In the case of the functionalized C-spheres, a broad peak observed around 3443 cm^{-1} could be attributed to the presence of −NH groups of the PEI polymer along with the −OH groups.[37,38] The small intensity peaks at 2922 and 2929 cm^{-1} belong to the C−H stretching vibrations indicating the presence of C−H bonds from the surface adsorbed PEI. The sharp peak near 1700 cm^{-1} corresponds to >C═O stretching.

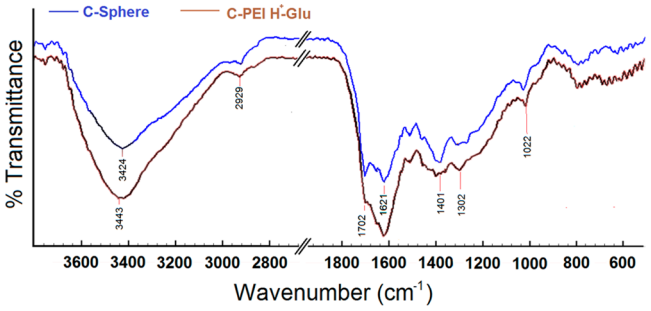

Figure 2. FT-IR spectra of C-spheres before and after modification for comparison.

The peak near 1620 cm^{-1} can be attributed to the −OH and −NH bending vibrations.[39] The peak at around 1400 cm^{-1} could be attributed to the presence of carboxylate groups −COO− at the surface of carbon spheres, which can get deprotonated after interaction with PEI. The appearance of a distinctive peak at 1300 cm^{-1} can be attributed to C−N stretch. The adsorption peak at 1025 and 1022 cm^{-1} can be assigned to the C−O stretching of alcohols or carboxylic acids.

The elemental analysis data of all materials used in this study are given in Table 1 for comparison. After the hydrothermal treatment, the percentage of carbon was increased considerably from 40% to 60.67% with simultaneous reduction in H content from 6.71% to 4.81%, which indicate significant carbonization of glucose.[26−28]

After coating the spheres with PEI, a significant amount of nitrogen (3.44%) was detected in the material. Presence of Cl (1.4%) after washing with 1 M HCl shows that only part of the imine nitrogen (18%) were protonated in the functionalized C -spheres.

A small amount of the carbonized materials was dispersed in water and deposited on a glass slide to investigate the morphology using SEM, which revealed the formation of C-spheres within the size range of 200−300 nm, as shown in Figure 3. After functionalization, there were no significant morphological changes in the material, and the spherical shape was retained indicating the robust nature of the C-spheres (Figure 3 and Figure S2, Supporting Information). The coating of PEI, followed by cross-linking with glutaraldehyde, stabilizes the PEI on the surface of C-spheres. After washing with 1 M HCl followed by water, the adsorbent was dried and used for the nanoparticle adsorption studies without further processing. The hydrodynamic radius, measured using a Zetasizer, was 340.0 ± 0.2 nm, whereas the zeta potential value was 25 ± 5 mV at normal pH (Figure S1, Supporting Information).

The pH of the medium is important for understanding the adsorption process as it influences the electrostatic interactions between the adsorbate and adsorbent.[40] To evaluate a favorable pH for the adsorption of NPs and to deduce the maximum adsorption capacity, NP solutions at different pH values were prepared. Ag and Au nanoparticle solutions were unstable at either acidic or basic pH (e.g., 2, 4, 10, and 12). Thus, the successive experiments were carried out at a pH range of 7−8.

Effects of Initial Pollutant Concentration and Contact Time. The unmodified C-spheres did not show any significant adsorption of NPs due to lack of favorable functional groups on the surface, which is shown in Figure S3 of the Supporting Information where we have used citrate-coated Ag NPs for the experiment. The adsorption capacity of the modified C-spheres with adsorption time for the NPs at 30 °C is given in Figure 4.

Table 1. Elemental Analysis of Modified C-spheres

materials	C (wt %)	H (wt %)	N (wt %)	O (wt %)	H/C	O/C	Cl (wt %)
glucose	40.00	6.71	–	53.29	0.168	1.33	–
C-sphere	64.67	4.81	<0.50	30.52	0.074	0.472	–
C-sphere_PEI	61.64	5.59	3.44	29.33	0.090	0.476	–
C-sphere_PEI_Glu	62.43	5.25	3.08	29.24	0.084	0.468	–
C-sphere_PEI_Glu_HCl	59.68	4.86	3.07	30.99	0.081	0.519	1.40

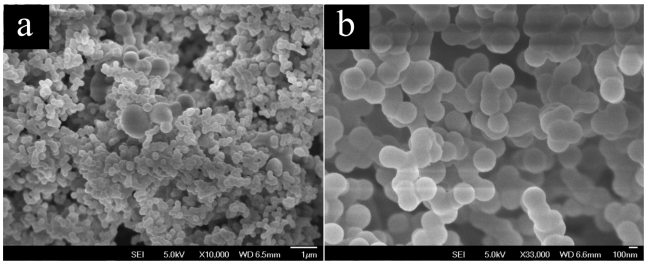

Figure 3. (a) Low- and (b) high-magnification FESEM images of functionalized C-spheres.

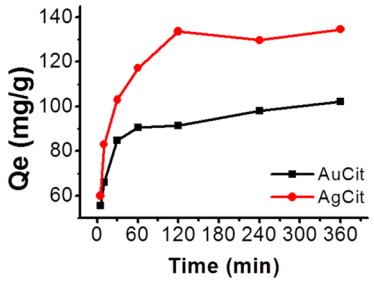

Figure 4. Variation of adsorption capacity of C-spheres with time for NPs at room temperature. (Conditions used: adsorbent = 2 mg; NP concentration = 50 ppm (AuNP) and 67 ppm (AgNP); volume = 9 mL). The concentration of nanoparticles in solution was determined using UV–vis spectroscopy measurements.

It is shown that the amount of NP adsorbed (mg/g) increased with time and reached an equilibrium. The adsorption of citrate-capped Ag NPs was higher compared to the AuCit NPs probably due to the favorable interaction of surface functional groups with AgNPs. The adsorption of NPs was monitored for 6 h to quantify the equilibrium adsorption capacity for each NP. The observed Q_e values of 134.5 and 102 mg/g for AgCit and AuCit NPs, respectively, are high compared to the reported values.[22,23] These results suggest that the protonated PEI-coated C-spheres (C-PEIH$^+$-Glu), with zeta potential of 21.3 ± 0.2 mV, serve as an excellent adsorbent for the removal of negatively charged NPs from water. TEM analysis of C-spheres (Figure 7) was done after adsorption of NPs to demonstrate the presence of NPs on the surface of C-spheres.

Adsorption Kinetics. Various kinetic models have been proposed in the literature addressing the adsorption of pollutants on adsorbent surface.[41−45] These models are crucial for the development of improved adsorbent materials and also give an insight into the adsorption mechanism. We have investigated the adsorption phenomenon of our functionalized C-spheres using different kinetic models, and pseudo-first-order (eq 2) and pseudo-second-order eqs (eq 3) are given below.

$$\text{Pseudo-first-order: } \log(Q_e - Q_t) = \log Q_t - \frac{K_1}{2.303}t \quad (2)$$

$$\text{Pseudo-second-order: } \frac{t}{Q_t} = \frac{1}{k_2 Q_e^2} + \frac{t}{Q_e} \quad (3)$$

where Q_e and Q_t indicate the amount of NPs adsorbed (mg/g) at equilibrium and at time t, respectively. The corresponding rate constants for the present adsorption are denoted by k_1 (min^{-1}) and k_2 (g mg^{-1} min). As shown in eq 2, a plot of $\log(Q_e - Q_t)$ vs t gave the first-order rate constants k_1 (slope) and experimental adsorption capacity Q_e (intercept), whereas a plot of $t/(Q_t)$ vs t from eq 3 gave the second-order rate constant k_2 (intercept) and experimental adsorption capacity Q_e (slope). Both time-dependent plots are given in Figure 5, and the corresponding values of various constants are listed in Table 2.

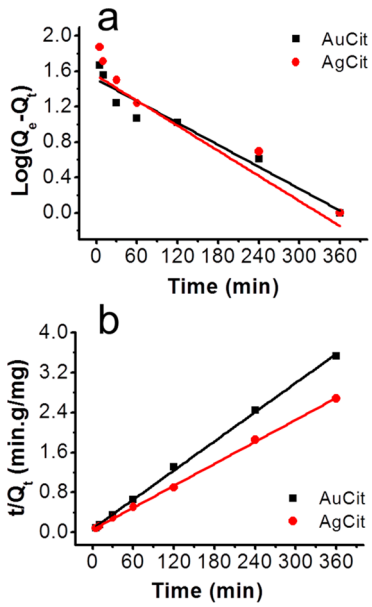

Figure 5. Pseudo-first-order kinetics (a) and pseudo-second-order kinetics (b) for the adsorption of nanoparticles by surface functionalized C-spheres.

The comparison of observed adsorption capacity with that of experimentally calculated values gives a clear idea about the adsorption mechanism. The adsorption mechanism of NPs can be best explained by pseudo-second-order kinetics as the correlation coefficients (R^2) for AuCit (0.999) and AgCit (0.9994) fits well with the experimental data compared to the pseudo-first-order kinetics where the R^2 values for AuCit (0.9446) and AgCit (0.6417) NPs deviates significantly from unity (Table 2). Further, the calculated adsorption capacities of 103 mg/g (AuNPs) and 137 mg/g (AgNPs) from the second-

Table 2. Pseudo-First-Order and Pseudo-Second-Order Constants and Correlation Coefficients for Adsorption of Different NPs on Functionalized C-spheres

	pseudo-first-order kinetics				pseudo-second-order kinetics		
	Q_e (mg g^{-1}) (experimental)	Q_e (mg g^{-1})	k_1 (min^{-1})	R^2	Q_e (mg g^{-1})	k^2 (g mg^{-1} min)	R^2
AgCit	135	53	1.08×10^{-2}	0.9643	137	9.6×10^{-4}	0.9994
AuCit	102	32	9.4×10^{-3}	0.9446	103	1.26×10^{-3}	0.999

order kinetics are in good agreement with the observed adsorption capacity of 102 (AuNPs) and 135 mg/g (AgNPs). The first-order adsorption capacity values are 32 mg/g (AuNPs) and 53 mg/g (AgNPs) (Table 2), which are much smaller than the calculated values. All these data indicated that the adsorption process followed the second-order adsorption kinetics. The extraction of NPs by adsorption process is not well understood. The purpose of using kinetic models is to understand different factors affecting the extraction efficiency. The NPs adsorption on PEI-modified C-spheres might involve one or a combination of electrostatic attraction, chemisorption, ion exchange, and complexation. It is not appropriate to conclude that the adsorption mechanism is based on two kinetic models. A proper mechanism can be explained only after complete understanding of adsorbent and adsorbate. This needs more theoretical and experimental analysis of NPs and adsorbent surfaces. We used conventional kinetic models to prove that the adsorption is not only due to diffusion but also due to chemisorption.

Adsorption Isotherm Studies. The adsorption isotherm studies were carried out for NP adsorption by the functionalized C-spheres to get a better understanding of the adsorption process. The adsorption of NPs was studied as a function of different concentration with time, and the data were used to determine the adsorption isotherm. The frequently studied Langmuir adsorption isotherm[46] and the Freundlich adsorption isotherm[47] were employed. The mathematical representations of Langmuir (eq 4) and Freundlich (eq 5) adsorption isotherm are given below:

$$\frac{C_e}{Q_e} = \left(\frac{1}{K_L}\right)Q_m + \frac{C_e}{Q_m} \tag{4}$$

$$\ln Q_e = \ln K_F + \frac{1}{n} \ln C_e \tag{5}$$

In the above equations, K_L and K_F represent the Langmuir and Freundlich constants, respectively, Q_e (mg g^{-1}) is the amount of NPs per unit gram, and C_e (mg L^{-1}) is the equilibrium concentration of NP in solution, whereas Q_m represents the theoretical monolayer adsorption capacity. A value of $1/n$ is also significant as its value below one indicates a normal Langmuir isotherm, while above one is indicative of cooperative adsorption.

The data obtained from the adsorption experiments are plotted in Figure 6. The Langmuir and Freundlich adsorption isotherm constants along with their correction coefficients are reported in Table 3. The linear graphical relationship indicate the applicability of Langmuir isotherm for the adsorption process as can be seen by the R^2 values for AuCit (0.9808) and AgCit (0.9928), which are close to unity as compared to the Freundlich isotherm (Table 3). Further, the value of $1/n$ (0.1505 for AuCit and 0.1801 for AgCit) is in accordance with the above observation.

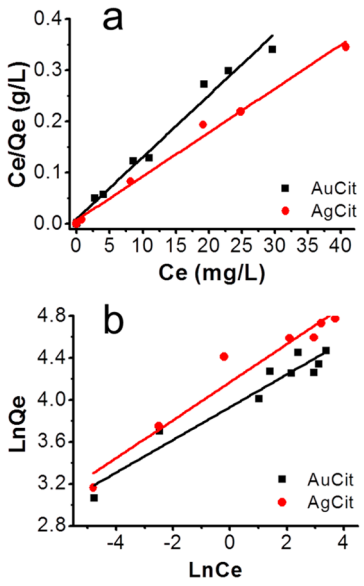

Figure 6. Langumir (a) and Freundlich isotherms (b) for the adsorption of AgCit NPS and AuCit NPS.

Another essential constant for Langmuir isotherm is known as separation factor (R_L), which is defined by eq 6.

$$R_L = \frac{1}{(1 + K_L C_e)} \tag{6}$$

This parameter dictates the shape of the isotherm depending on the following characteristics: $R_L > 1$ is unfavorable adsorption; $R_L = 1$ corresponds to a linear isotherm; $0 < RL < 1$ is favorable and $R_L = 0$ is irreversible. The R_L values for the adsorption of AuCit (0.0151) and AgCit (0.012) on the C-spheres indicate a favorable adsorption process (Table 3).

It is understood that the coating of PEI onto the C-spheres occurred through the adsorption process, and leaching of PEI from the surface into the extraction medium was prevented by cross-linking with glutaraldehyde to reduce the solubility of PEI in water. The adsorption of NPs on PEI-modified C-spheres was facilitated by the electrostatic interaction between the negatively charged nanoparticles and positively charged C-spheres. The observed extraction efficiency for AgNPs was much higher than AuNPs. The free amino groups also provide favorable binding interaction through coordination to the nanoparticle surface.

Characterization of Adsorbent Surface after Extraction. The modified C-spheres after the NP adsorption were analyzed using SEM, which showed the presence of Au and Ag NPs on the surface, which is also identified by the EDS analysis (Figure 7). The homogeneous dispersion of NPs on the surface with no significant morphological changes of the C-spheres after adsorption of NPs demonstrate the stability of the C-spheres and affinity toward negatively charged NPs. In order to check that NPs possess the known catalytic activity after

dx.doi.org/10.1021/sc5004242 | ACS Sustainable Chem. Eng. 2014, 2, 2675−2682

Table 3. Langmuir and Freundlich Isotherm Constants and Correlation Coefficients for Adsorption of Nanoparticles on Functionalized C-spheres

	Langmuir Constants				Freundlich Constants		
	Q_m (mg/g)	K_L (L g^{-1})	R_L	R^2	K_F (mg g^{-1}) (L g^{-1})^n	$1/n$	R^2
AgCit	116	1.2286	0.0120	0.9928	64.845	0.1801	0.9474
AuCit	83	1.3011	0.0151	0.9808	50.978	0.1557	0.935

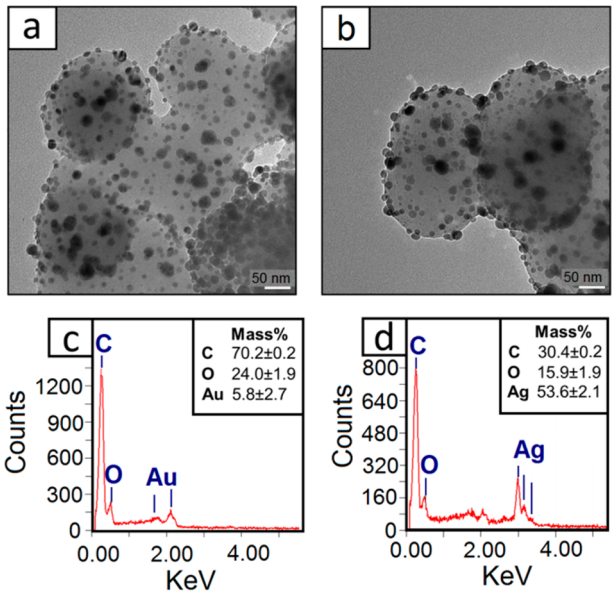

Figure 7. TEM images of C-spheres after adsorption of (a) AuCit and (b) AgCit NPs and corresponding EDS data of functionalized C-spheres after adsorption of (c) AuCit and (d) AgCit NPs.

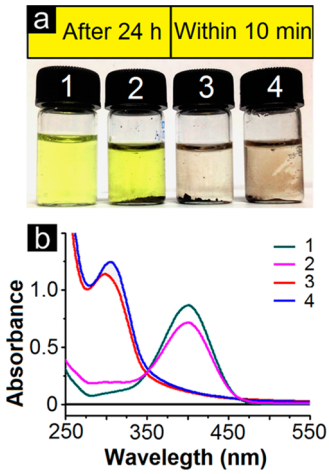

Figure 8. (a) Images showing the reduction of *p*-NP by Au and Ag NPs adsorbed on C-spheres in the presence of $NaBH_4$. (b) Corresponding UV–vis spectra for *p*-NP reduction ([$NaBH_4$] = 0.1 M and [*p*-NP] = 1.0×10^{-4} M; **1** = *p*-NP/$NaBH_4$; **2** = *p*-NP/$NaBH_4$/C-sphere; **3** = *p*-NP/$NaBH_4$/AgCit@C-sphere; **4** = *p*-NP/$NaBH_4$/AuCit@C-sphere. UV–vis spectra of **1** and **2** were recorded after diluting the solution four times compared to the UV–vis spectra of **3** and **4**, which were used as such).

adsorption and to find potential applications of nanoparticles adsorbed on C-spheres, a few catalytic reactions have been carried out.

***p*-Nitrophenol Reduction.** Catalytic activities of AuNPs and AgNPs have been reported by many research groups. To check the activity of metal nanoparticles adsorbed on the C-sphere surface, a well-studied reduction of the *p*-nitrophenol (*p*-NP) reaction was selected.[48−50] Small quantities of Au NPs or Ag NPs adsorbed on C-spheres (0.02 g) obtained from the extraction experiment were suspended in an aqueous solution of *p*-NP/$NaBH_4$ (2.0 mL − [$NaBH_4$] = 0.1 M and [*p*-NP] = 1.0×10^{-4} M) and stirred, and the progress of the reaction was monitored using a UV–vis spectrophotometer. The reducing agent, $NaBH_4$, is not capable of reducing *p*-NP even after 24 h, whereas after the addition of AgCit/C or AuCit/C as a catalyst, the reaction was completed within 10 min as indicated by the absence of a yellow color (Figure 8a). The UV–vis spectra also showed the disappearance of a peak at 400 nm (λ_{max}), which is associated with *p*-NP with the generation of a new peak at 300 nm associated with *p*-amino phenol, the reduced product (Figure 8b).

A few control experiments such as *p*-nitrophenol reduction under different conditions such as stirring with $NaBH_4$ alone or with C-spheres and NaBH4 with no NPs led to no detectable product formation in the reaction mixture. The small decrease in the intensity could be attributed to the adsorption of *p*-NP on C-spheres rather than reduction (Figure 8b). Both the reducing agent and the nanoparticles on the C-spheres are needed for the successful reduction of $-NO_2$ groups to $-NH_2$ groups. The catalytic nature of *p*-NP reduction was established by using the same material (NP@C-spheres) for three successive reductions (data not shown). In summary, the PEI-coated C-spheres are excellent adsorbents for metal NPs, and C-spheres with NPs on the surface can be used as catalysts for chemical transformations.

CONCLUSION

A low-temperature hydrothermal carbonization route was applied to generate C-spheres from glucose. The post-modification of the C-sphere surface includes adsorption of PEI, cross-linking with glutaraldehyde, and protonation with dilute acid. Surface-modified C-spheres were used for the extraction of citrate-capped Au and Ag NPs. The synthesized material showed excellent adsorption capacity of 102 mg/g (AuNPs) and 135 mg/g (AgNPs). Among the isotherm models tested, Langmuir adsorption fits well with the adsorption data as indicated by the R^2 values, 0.9928 and 0.9808 for Ag and AuCit NPs, respectively. Kinetic studies showed that the adsorption for both the NPs followed the pseudo-second-order model as the calculated Q_e values (103 and 137 mg/g for Ag and AuCit NPs, respectively) were close to the experimental values, and the R^2 values were close to unity (0.9994 and 0.999 for Ag and AuCit NPs, respectively). Various factors such as size, surface charge, and interaction of functional groups on the adsorbent surface are responsible for the different extraction capacities. Ligand–metal interactions based on the hard–soft acid–base (HSAB) theory along with electrostatic interactions could be the possible explanation for the higher extraction capacity of Ag NPs. Catalytic activity of adsorbed NPs was examined for the reduction of p-nitrophenol, which showed fast

dx.doi.org/10.1021/sc5004242 | ACS Sustainable Chem. Eng. 2014, 2, 2675−2682

reduction within 10 min to form *p*-aminophenol. The synthesis and use of such carbonized materials are simple and cost effective and offers an efficient method for water treatment. It is conceivable that the material developed here can offer an environmentally friendly and cheaper way of removing nanoparticles from the water supply.

■ ASSOCIATED CONTENT

Supporting Information

Synthetic scheme for the carbon material and characterization data. This material is available free of charge via the Internet at http://pubs.acs.org.

■ AUTHOR INFORMATION

Corresponding Author

*E-mail: chmsv@nus.edu.sg.

Present Address

A. Adin is currently visiting from Hebrew University of Jerusalem, Israel

Notes

The authors declare no competing financial interest.

■ ACKNOWLEDGMENTS

The authors thank the Environment and Water Industry Programme Office (EWI) under the National Research Foundation of Singapore, NUS Environmental Research Institute, and National University of Singapore (PUBPP 21100/36/2, NUS WBS no. R-706-002-013-290, R-143-000-458-750, R-143-000-458-731) for the financial support of the work. Also technical support from Department of Chemistry, NUS Environmental Research Institute, and Department of Chemistry, National University of Singapore is acknowledged.

■ REFERENCES

(1) Alivisatos, P. The use of nanocrystals in biological detection. *Nat. Biotechnol.* **2004**, *22*, 47−52.

(2) Hasan, J.; Crawford, R. J.; Ivanova, E. P. Antibacterial surfaces: The quest for a new generation of biomaterials. *Trends Biotechnol.* **2013**, *31*, 295−304.

(3) Dror-Ehre, A.; Adin, A.; Markovich, G.; Mamane, H. Control of biofilm formation in water using molecularly capped silver nanoparticles. *Water Res.* **2010**, *8*, 2601−2609.

(4) Klaine, S. J.; Alvarez, P. J. J.; Batley, G. E.; Fernandes, T. F.; Handy, R. D.; Lyon, D. Y.; Mahendra, S.; McLaughlin, M. J.; Lead, J. R. Nanomaterials in the environment: Behavior, fate, bioavailability, and effects. *Environ. Toxicol. Chem.* **2008**, *27*, 1825−1851.

(5) Lowry, G. V.; Espinasse, B. P.; Badireddy, A. R.; Richardson, C. J.; Reinsch, B. C.; Bryant, L. D.; Bone, A. J.; Deonarine, A.; Chae, S.; Therezien, M.; Colman, B. P.; Hsu-Kim, H.; Bernhardt, E. S.; Matson, C. W.; Wiesner, M. R. Long-term transformation and fate of manufactured Ag nanoparticles in a simulated large scale freshwater emergent wetland. *Environ. Sci. Technol.* **2012**, *46*, 7027−7036.

(6) Levard, C.; Hotze, E. M.; Lowry, G. V.; Brown, G. E., Jr. Environmental transformations of silver nanoparticles: Impact on stability and toxicity. *Environ. Sci. Technol.* **2012**, *46*, 6900−6914.

(7) Musee, N. Nanowastes and the environment: Potential new waste management paradigm. *Environ. Int.* **2011**, *37*, 112−128.

(8) Nowack, B.; Ranville, J. F.; Diamond, S.; Gallego-Urrea, J. A.; Metcalfe, C.; Rose, J.; Horne, N.; Koelmans, A. A.; Klaine, S. J. Potential scenarios for nanomaterial release and subsequent alteration in the environment. *Environ. Toxicol. Chem.* **2012**, *31*, 50−59.

(9) Benn, T.; Cavanagh, B.; Hristovski, K.; Posner, J. D.; Westerhoff, P. The release of nanosilver from consumer products used in the home. *J. Environ. Qual.* **2010**, *39*, 1875−1882.

(10) Gottschalk, F.; Nowack, B. The release of engineered nanomaterials to the environment. *J. Environ. Monit.* **2011**, *13*, 1145−1155.

(11) Ferry, J. L.; Craig, P.; Hexel, C.; Sisco, P.; Frey, R.; Pennington, P. L.; Fulton, M. H.; Scott, I. G.; Decho, A. W.; Kashiwada, S.; Murphy, C. J.; Shaw, T. J. Transfer of gold nanoparticles from the water column to the estuarine food web. *Nat. Nanotechnol.* **2009**, *4*, 441−444.

(12) Teow, Y.; Asharani, P. V.; Hande, M. P.; Valiyaveettil, S. Health impact and safety of engineered nanomaterials. *Chem. Commun.* **2011**, *47*, 7025−7038.

(13) Asare, N.; Instanes, C.; Sandberg, W. J.; Refsnes, M.; Schwarze, P.; Kruszewski, M.; Brunborg, G. Cytotoxic and genotoxic effects of silver nanoparticles in testicular cells. *Toxicology* **2012**, *291*, 65−72.

(14) Navarro, E.; Baun, A.; Behra, R.; Hartmann, N. B.; Filser, J.; Miao, A. J.; Quigg, A.; Santschi, P. H.; Sigg, L. Environmental behavior and ecotoxicity of engineered nanoparticles to algae, plants, and fungi. *Ecotoxicology* **2008**, *17*, 372−386.

(15) Weinberg, H.; Galyean, A.; Leopold, M. Evaluating engineered nanoparticles in natural waters. *TrAC, Trends Anal. Chem.* **2011**, *30*, 72−83.

(16) Fabrega, J.; Luoma, S. N.; Tyler, C. R.; Galloway, T. S.; Lead, J. R. Silver nanoparticles: Behaviour and effects in the aquatic environment. *Environ. Int.* **2011**, *37*, 517−531.

(17) Li, H.; Gui, X.; Zhang, L.; Wang, S.; Ji, C.; Wei, J.; Wang, K.; Zhu, H.; Wu, D.; Cao, A. Carbon nanotube sponge filters for trapping nanoparticles and dye molecules from water. *Chem. Commun.* **2010**, *46*, 7966−7968.

(18) Hou, L.; Li, K.; Ding, Y.; Li, Y.; Chen, J.; Wu, X.; Li, X. Removal of silver nanoparticles in simulated wastewater treatment processes and its impact on COD and NH(4) reduction. *Chemosphere* **2012**, *87*, 248−252.

(19) Liu, Y.; Tourbin, M.; Lachaize, S.; Guiraud, P. Nanoparticles in wastewaters: Hazards, fate and remediation. *Powder Technol.* **2014**, *255*, 149−156.

(20) Khan, S. S.; Mukherjee, A.; Chandrasekaran, N. Adsorptive removal of silver nanoparticles (SNPs) from aqueous solution by *Aeromonas punctata* and its adsorption isotherm and kinetics. *Colloids Surf., B* **2012**, *92*, 156−160.

(21) Ladner, D. A.; Steele, M.; Weir, A.; Hristovski, K.; Westerhoff, P. Functionalized nanoparticle interactions with polymeric membranes. *J. Hazard. Mater.* **2012**, *212*, 288−95.

(22) Mahanta, N.; Leong, W. Y.; Valiyaveettil, S. Isolation and characterization of cellulose-based nanofibers for nanoparticle extraction from an aqueous environment. *J. Mater. Chem.* **2012**, *22*, 1985−1993.

(23) Mahanta, N.; Valiyaveettil, S. Surface modified electrospun poly(vinyl alcohol) membranes for extracting nanoparticles from water. *Nanoscale* **2011**, *3*, 4625−4631.

(24) Gicheva, G.; Yordanov, G. Removal of citrate-coated silver nanoparticles from aqueous dispersions by using activated carbon. *Colloids Surf., A* **2013**, *431*, 51−59.

(25) Hu, B.; Wang, K.; Wu, L.; Yu, S.-H.; Antonietti, M.; Titirici, M.-M. Engineering Carbon Materials from the Hydrothermal Carbonization Process of Biomass. *Adv. Mater.* **2010**, *22*, 813−828.

(26) Liu, S.; Sun, J.; Huang, Z. Carbon spheres/activated carbon composite materials with high Cr(VI) adsorption capacity prepared by a hydrothermal method. *J. Hazard. Mater.* **2010**, *173*, 377−383.

(27) Sevilla, M.; Fuertes, A. B. Chemical and structural properties of carbonaceous products obtained by hydrothermal carbonization of saccharides. *Chem.—Eur. J.* **2009**, *15*, 4195−4203.

(28) Li, M.; Li, W.; Liu, S. Hydrothermal synthesis, characterization, and KOH activation of carbon spheres from glucose. *Carbohyd. Res.* **2011**, *346*, 999−1004.

(29) Wang, X.; Liu, J.; Xu, W. One-step hydrothermal preparation of amino-functionalized carbon spheres at low temperature and their enhanced adsorption performance towards Cr(VI) for water purification. *Colloids Surf., A* **2012**, *415*, 288−294.

(30) Guan, Z.; Liu, L.; He, L.; Yang, S. Amphiphilic hollow carbonaceous microspheres for the sorption of phenol from water. *J. Hazard. Mater.* **2011**, *196*, 270−277.
(31) Mallampati, R.; Valiyaveettil, S. Application of tomato peel as an efficient adsorbent for water purification-alternative biotechnology? *RSC Adv.* **2012**, *2*, 9914−9920.
(32) Mallampati, R.; Valiyaveettil, S. Simple and efficient biomimetic synthesis of Mn3O4 hierarchical structures and their application in water treatment. *J. Nanosci. Nanotechnol.* **2012**, *12*, 618−622.
(33) Polte, J.; Ahner, T. T.; Delissen, F.; Sokolov, S.; Emmerling, F.; Thünemann, A. F.; Kraehnert, R. Mechanism of gold nanoparticle formation in the classical citrate synthesis method derived from coupled in situ XANES and SAXS evaluation. *J. Am. Chem. Soc.* **2010**, *132*, 1296−1301.
(34) Van Hyning, D. L.; Zukoski, C. F. Formation mechanisms and aggregation behavior of borohydride reduced silver particles. *Langmuir* **1998**, *14*, 7034−7046.
(35) Mpourmpakis, G.; Vlachos, D. G. Insights into the early stages of metal nanoparticle formation via first-principle calculations: The roles of citrate and water. *Langmuir* **2008**, *24*, 7465−7473.
(36) Farooq, U.; Kozinski, J. A.; Khan, M. A.; Athar, M. Biosorption of heavy metal ions using wheat based biosorbents–A review of the recent literature. *Bioresour. Technol.* **2010**, *101*, 5043−5053.
(37) Ashokan, A.; Menon, D.; Nair, S.; Koyakutty, M. A molecular receptor targeted, hydroxyapatite nanocrystal based multi-modal contrast agent. *Biomaterials* **2010**, *31*, 2606−2616.
(38) Chang, Q.; Wang, G. Study on the macromolecular coagulant PEX which traps heavy metals. *Chem. Eng. Sci.* **2007**, *62*, 4636−4643.
(39) Barone, P. W.; Baik, S.; Heller, D. A.; Strano, M. S. Near-infrared optical sensors based on single-walled carbon nanotubes. *Nat. Mater.* **2005**, *4*, 86−92.
(40) Salleh, M. A. M.; Mahmoud, D. K.; Karim, W. A. W. A.; Idris, A. Cationic and anionic dye adsorption by agricultural solid wastes: A comprehensive review. *Desalination* **2011**, *280*, 1−13.
(41) Volesky, B. Biosorption and me. *Water Res.* **2007**, *41*, 4017−4029.
(42) Aksu, Z. Application of biosorption for the removal of organic pollutants: a review. *Process Biochem.* **2005**, *40*, 997−1026.
(43) Febrianto, J.; Kosasih, A. N.; Sunarso, J.; Ju, Y. H.; Indraswati, N.; Ismadji, S. Equilibrium and kinetic studies in adsorption of heavy metals using biosorbent: A summary of recent studies. *J. Hazard. Mater.* **2009**, *162*, 616−645.
(44) Sen Gupta, S.; Bhattacharyya, K. G. Kinetics of adsorption of metal ions on inorganic materials: A review. *Adv. Colloid Interfac.* **2011**, *162*, 39−58.
(45) Park, D.; Yun, Y.-S.; Park, J. The past, present, and future trends of biosorption. *Biotechnol. Bioproc. E* **2010**, *15*, 86−102.
(46) Langmuir, I. The adsorption of gases on plane surfaces of glass, mica and platinum. *J. Am. Chem. Soc.* **1918**, *40*, 1361−1403.
(47) Freundlich, H. M. F. Uber die adsorption in losungen. *Z. Phys. Chem.* **1906**, *57*, 385−470.
(48) Mondal, K.; Kumar, J.; Sharma, A. Self-organized macroporous thin carbon films for supported metal catalysis. *Colloids Surf., A* **2013**, *427*, 83−94.
(49) Saha, S.; Pal, A.; Kundu, S.; Basu, S.; Pal, T. Photochemical green synthesis of calcium-alginate-stabilized Ag and Au nanoparticles and their catalytic application to 4-nitrophenol reduction. *Langmuir* **2009**, *26*, 2885−2893.
(50) Wunder, S.; Polzer, F.; Lu, Y.; Mei, Y.; Ballauff, M. Kinetic analysis of catalytic reduction of 4-nitrophenol by metallic nanoparticles immobilized in spherical polyelectrolyte brushes. *J. Phys. Chem. C* **2010**, *114*, 8814−8820.